Journal of Physics and Chemistry of Solids 180 (2023) 111414

Contents lists available at ScienceDirect

Journal of Physics and Chemistry of Solids

journal homepage: www.elsevier.com/locate/jpcs

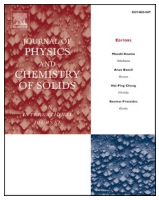

Structuring thermal transport in pristine graphene with h-BN nanorings

Dan Tan [a], Morten Willatzen [b,*], Johan Christensen [c,**]

[a] School of Advanced Materials and Nanotechnology, Xidian University, Xi'an, China
[b] Beijing Institute of Nanoenergy and Nanosystems, Chinese Academy of Sciences, Beijing, PR China
[c] IMDEA Materials Institute, Calle Eric Kandel, 2, 28906, Getafe, Madrid, Spain

ARTICLE INFO

Keywords:
Structuring graphene
Thermal conductivity
Molecular dynamics
Green-kubo simulations
Electric field

ABSTRACT

Structuring graphene has led to a wealth of opportunities to enhance or at least to alter its electronic, optical and thermal properties. E.g, punching holes in graphene in the form antidot lattices turns the base material from a semimetal into a semiconductor. In here, we aim at leaving graphene pristine, but instead growing h-BN nanorings on top of it with the desire to alleviate heat spread by virtue of a reduced thermal conductivity. By combining empirical molecular dynamics and Green-Kubo simulations, we predict that using thinner nanorings leads to rapidly decaying heat currents and therefore remarkably reduced thermal conductivities by 76% in comparison to graphene. Interestingly, we also argue how an applied electric field breaks the underlying crystal symmetry enabling directionally tunable thermal transport. We foresee exciting possibilities to subdue optical and plasmonic loss channels by reduced thermal dissipation.

1. Introduction

Ever since graphene was lifted of a block of graphite using only a piece of Scotch tape, the excitement behind this atomically thin layer seems not to cease [1]. The unique electronic, mechanical, and optical properties of graphene have spurred enormous interest [2–4], from which applications such as optical sensors, transparent electrodes, NEMs, and plasmonic light guiding are rapidly emerging [5–7]. Also, a rapidly growing nanotechnology frontier is that of van der Waals heterostructures, wherein stacks of atomically thin materials, not limited to graphene, are assembled to form a complex quantum metamaterial [8,9].

Engineering the thermal transport in graphene is as well a thriving frontier, thanks to its extraordinary capability to conduct heat and thermal transport in general. According to earlier papers, the measured thermal conductivity (TC) of graphene is in the range of 3000–5000 W/mK at room temperature, which can be considered remarkably high when compared to its base-bulk material [10–12]. On the contrary, the prospect of reducing or alleviating heat spread or dissipation, has and still is the main driving force behind growing activities to employ phononic crystals and nanophononic metamaterials with the aim to reduce the TC [13]. One of the ultimate goals in this arena is the desire to improve optical, electronical, and plasmonic devices by deliberately suppressing the dissipative channels caused by thermal losses. Through phonon engineering in both its long and short wavelength regime; band-flattening approaches, superlattice designs, phonon interference, and anisotropic boundary scattering, have all led to a wealth of opportunities to craft the flow of heat [14–18]. Despite these inventive approaches, in contrast to synthesizing man-made thermal properties by the use of superlattices or nanophononic metamaterials that alter the very base material, and by the same token, inevitably, changes the electrical and mechanical properties, it is highly desired to render the material pristine. Due to the extremely low lattice mismatch of 1.7%, graphene/h-BN heterostructures are found to be powerful candidates for graphene-based devices. Many studies prove that the properties like phonon dispersion [19], electrical conductivity [20], band structure [21] are different from pristine graphene and h-BN.

In this paper, we decorate pristine graphene sheets with h-BN nanorings to alter the TC of graphene, by virtually leaving it intact, i.e., otherwise unstructured and undoped. We carried out empirical molecular dynamics simulations to calculate the thermal conductivity using the equilibrium Green-Kubo formalism. By engineering a number of nanorings-structured graphene sheets of varying outer radius, we predict that the heat current auto-correlation function (HCACF), accordingly, undergoes a reduction both with time and temperature, which is responsible for the reported heat alleviation, i.e., the decrease of the TC.

* Corresponding author.
** Corresponding author.
E-mail addresses: mortenwillatzen@binn.cas.cn (M. Willatzen), johan.christensen@imdea.org (J. Christensen).

https://doi.org/10.1016/j.jpcs.2023.111414
Received 6 February 2023; Received in revised form 16 April 2023; Accepted 30 April 2023
Available online 16 May 2023

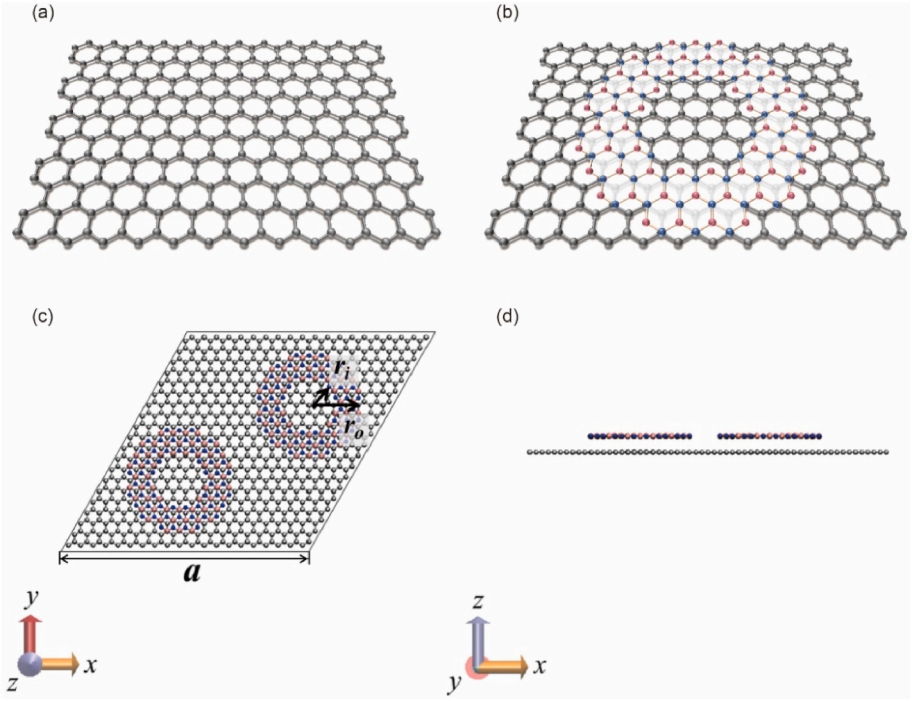

Fig. 1. The simulation model of (a) pristine graphene and (b) h-BN nanorings on graphene.(c) Top view and (d) side view of the simulation unit cells for pristine graphene and h-BN nanorings on graphene. Black, pink, and blue spheres represent carbon boron, and nitrogen atoms, respectively.

Further, for the first time, we also discuss how an applied electric field breaks the underlying crystal symmetry enabling directionally tunable thermal transport. We foresee that the ability to tune the TC of graphene without the need to alter it, should have substantial importance in future devices where unintentional electronic or optical modifications are absent from improved thermal characteristics.

2. Theory

We carried out empirical molecular dynamics (EMD) simulation of two-dimensional periodic structures with a super-cell consisting of a monolayer of graphene upon which rings of graphene-like h-BN are grown as depicted in Fig. 1 [22,23]. Each triclinic primitive cell consists of h-BN nanorings whose inner radii r_i are the same, 4.0 Å. For different outer radii r_o = 10.0 Å, 9.3 Å, and 7.9 Å, respectively, the number of atoms in each h-BN nanorings are 114, 84, 72, respectively. The graphene substrate contains 800 atoms in each unitcell. The lattice constant a is 50.44 Å. The effective distance between h-BN and graphene layer along z axis is 3.4 Å.

Generally speaking, the TC κ of a material describes the proportionality between the heat flux **J** and the temperature gradient according to Fourier's law, which is written as

$$\mathbf{J} = -\kappa(T)\cdot\nabla T, \tag{1}$$

where T is the temperature. For typical solids, the dominant contribution to the TC stems from lattice vibrations (phonons). In our simulations, the TC tensor $\kappa_{\alpha\beta}$ was obtained using the Green-Kubo formula

$$\kappa_{\alpha\beta} = \frac{1}{k_B V T^2}\int_0^\infty < J_\alpha(t)J_\beta(0) > dt, \tag{2}$$

where k_B is Boltzmann's constant, V is the volume of the super-cell, and $< J_\alpha(t)J_\beta(0) >$ is the ensemble average of the heat current autocorrelation (HCACF). It follows from hexagonal symmetry that the heat conductivity tensor obeys

$$\kappa_{\alpha\beta} = \kappa\delta_{\alpha\beta}, \tag{3}$$

where $\delta_{\alpha\beta}$ is a Kronecker delta. Our EMD calculations confirm this group symmetry result.

3. Simulation details

All of the MD simulations are performed using the LAMMPS computational package [24]. The Tersoff potential is used to describe the intralayer interactions for graphene and BN [25,26], while the interlayer interactions are described using the potential ILP [27,28]. It should be noted that LAMMPS calculates heat current expressions using two-body potentials rather than more accurate many-body potentials [29]. However, it is still expected that the overall trends in heat current calculations are captured well by LAMMPS. In our simulations, the conjugate gradient method is used to ensure that the total energy reaches a local minimum. Then, the obtained energy-minimized structure is relaxed for 1 ns to reach equilibrium by applying a Langevin thermostat in conjunction with a constant-volume, constant-energy (NVE) ensemble. The heat current data are recorded in every ten steps by performing constant energy simulations for 20 ns. The heat flux autocorrelation values are calculated by averaging ten obtained HCACFs. A fixed time step of 2 fs is used throughout the simulations. Molecular dynamics simulations were performed with a triclinic box containing 3 × 3 × 1 unit cells where no significant simulation domain size effect is found. When calculating the 2D structure's volume, its thickness is measured as the distance between the 1/2 heights of two gaps in trilayer structures. Fig. S1 shows the detailed diagram how to measure the thickness. Here the thickness is 6.7 Å for our 2D structure. Periodic boundary conditions are imposed along the x and y directions. A 40 Å vacuum layer is set perpendicularly to avoid interlayer interactions. The effect of external electric field is also discussed, which is applied by adding a force $\mathbf{F} = q\mathbf{E}$ to each charged atom during the simulation. The charges for Boron, Nitrogen atoms are determined according to Ref [30], which are 0.907, −0.907, respectively. Carbon charge is set as 0 to keep the body electrically neutral. All the parameters were verified through

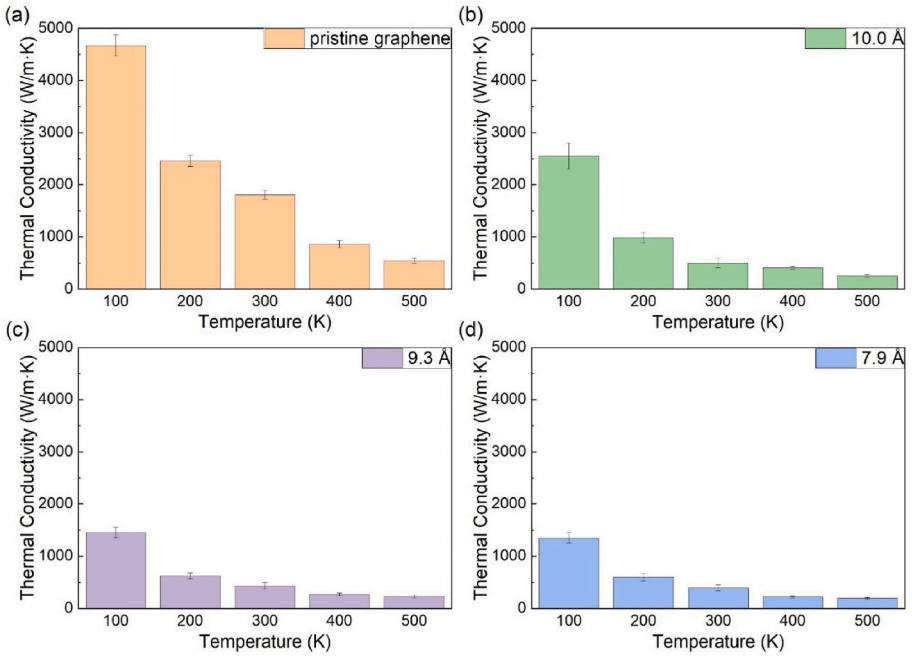

Fig. 2. Thermal conductivities at different temperatures of (a) pristine graphene and h-BN nanorings on a graphene substrate with three different outer radii (b) 10 Å, (c) 9.3 Å, and (d) 7.9 Å.

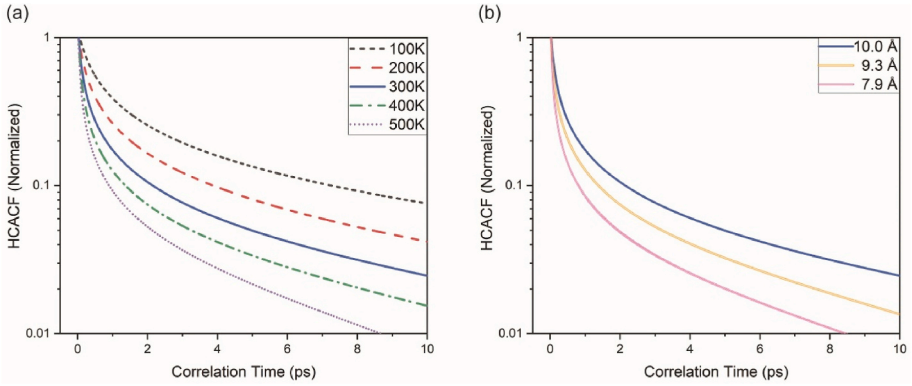

Fig. 3. The integrand $< J_\alpha(t)J_\beta(0) >$ of the thermal conductivity κ corresponding to (a) a h-BN nanoring of 10 Å on a graphene substrate at different temperatures, and (b) h-BN nanorings on a graphene substrate with three different outer radii (all at $T = 300$ K).

crystal structure and phonon dispersion relation of h-BN layer on graphene layer. Fig. S2 shows the phonon dispersion curves of the top h-BN layer, the bottom graphene layer, and the whole structure, respectively.

4. Results

In Fig. 2, the calculated TC (κ) is shown as a histogram vs. temperature for three examples comprising h-BN ring-patterned graphene as well as the pristine graphene case. In all four examples, TC decreases significantly with increasing temperature due to two factors: the appearance of T^2 in the denominator of Eq. (2) and the variation of HCACF with temperature. In all cases, we predict a TC reduction compared to pristine graphene. Interestingly, the thinner the h-BN rings are, the more pronounced the reduction in TC is. For example, at room temperature the TC of the h-BN ring structure on graphene with outer radius 7.9 Å [Fig. 2d] shrinks by 76% compared to graphene.

To understand the behaviour of TC better, we next plot the integrand HCACF as function of the correlation time t for different temperatures in Fig. 3a. Evidently, HCACF decays rapidly both as function of t and temperature T. In Fig. 3b, the temporal evolution of HCAC at 300K is plotted for different outer radii. In agreement with the tendency discussed in Fig. 2, the thinner the h-BN nanorings are, the stronger the decay of HCAC is.

For our hexagonal structure, the thermal conductivity κ obeys the same symmetry as the permittivity ε since they both couple two vectors: $\mathbf{J} = \kappa\nabla T$ (thermal conductivity) and $\mathbf{D} = \varepsilon\mathbf{E}$ (permittivity). Hence, in hexagonal structures the thermal conductivity tensor is isotropic in the plane perpendicular to the hexagonal c direction, that is $\kappa_{xx} = \kappa_{yy}$, while κ_{zz} is generally different from κ_{xx} (κ_{yy}). Our calculated results using EMD statistics calculations shown in Fig. 4 indeed verify this symmetry. Here, a large maximum correlation time of $t_{max} = 20$ns is considered, while ten independent simulations from NVE ensemble are conducted to show the correlation time-dependent κ (grey thin lines). The ensemble averaged curves show the calculated TC components at a fixed temperature (green thick lines). Since these figures shown good convergence after 10 ps, the in-plane TC results are obtained as $(\kappa_{xx} + \kappa_{yy})/2$ between 10 ps and 20 ps for correlation time, where the standard error on mean is presented as error bar in Fig. 2.

Having demonstrated that temperature is a control parameter for TC, we now examine how an external electric field can be applied to tune

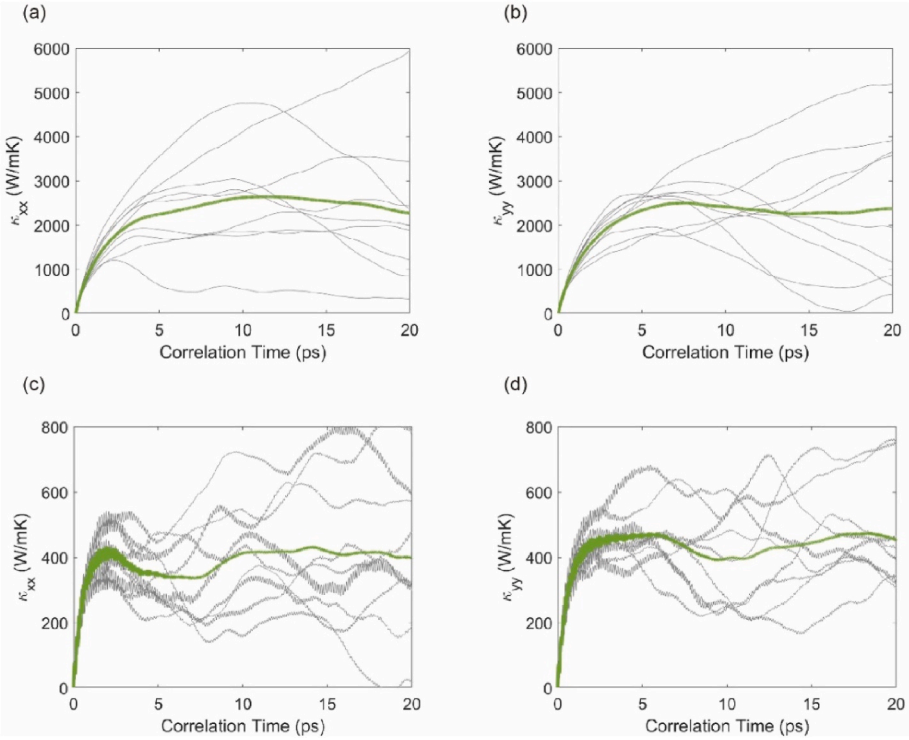

Fig. 4. Averaged TC curves (green thick lines) κ_{xx}, κ_{yy} of (a, b) pristine graphene and (c, d) a h-BN nanoring of 10 Å on a graphene substrate from ten independent NVE ensembles (grey thin lines).

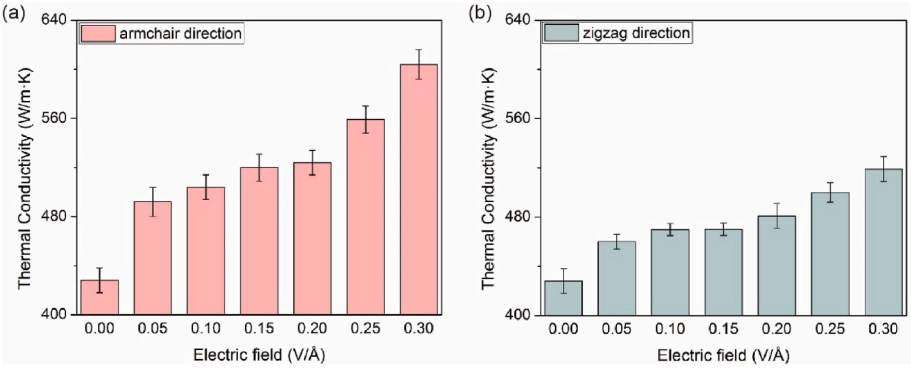

Fig. 5. In-plane thermal conductivity of the h-BN ring-patterned graphene under different external electric field along (a) armchair direction and (b) zigzag direction.

TC. This is demonstrated by adding an in-plane electric field along the armchair (x) and zigzag (y) directions to both pristine graphene and the h-BN ring-patterned graphene. The in-plane TC results are obtained as $(\kappa_{xx} + \kappa_{yy})/2$. In the case of pristine graphene, there is nearly no effect while the effect on h-BN ring-patterned graphene is shown in Fig. 5. For h-BN ring-patterned graphene, an external electric enhances TC but the enhancement factor is larger when the electric field is applied along the armchair direction compared to the zigzag direction. The enhancement factor is 1.41 (1.21) along the armchair (zigzag) direction at an electric field of 0.30 V/Å. Besides, the TC tensor becomes anisotropic when applying external electric field. Fig. S3 shows the averaged TC curves κ_{xx} and κ_{yy} of the h-BN ring-patterned graphene under external electric field of 0.3 V/Å along armchair direction. We can see that unlike the former results in Fig. 4, here the κ_{xx} differs from κ_{yy}. The main reason is a strain-effected crystal-symmetry breaking induced by piezoelectricity when an electric field is imposed.

Our h-BN ring-patterned graphene belongs to the $\bar{6}m2$ symmetry group whose piezoelectric strain matrix is,

$$d_{ij} = \begin{bmatrix} d_{x1} & -d_{x1} & 0 & 0 & 0 & 0 \\ 0 & 0 & 0 & 0 & 0 & -2d_{x1} \\ 0 & 0 & 0 & 0 & 0 & 0 \end{bmatrix} \quad (4)$$

When adding an electric field E, a strain S is induced,

$$[S_j] = [d_{ij}]^T \cdot [E_k] . (i,k = 1,2,3; j = 1,2 \ldots 6) \quad (5)$$

Thus, normal strain components $S_1 = S_{xx}$ and $S_2 = S_{yy}$ are generated when an $E_1 = E_x$ electric field component is applied. When an electric field $E_2 = E_y$ is applied, the induced strain is shear, $S_6 = 2S_{xy}$. This explains why the TC tuning effect is more pronounced when applying an electric field along the x direction compared to the y direction. Indeed, the morphological change is larger in the case of a normal strain compared to a shear strain. For non-piezo pristine graphene, the morphological change is zero, hence there is no effect from external electric effect.

In general, there are different strategies to tune TC. The TC of light-responsive materials such as azobenzene polymer can be tuned using a

light-triggered thermal conductivity switching method. Here, the π-π stacking geometry is altered which can lead to a crystal-to-liquid transition [31]. Temperature regulation of TC is another way to establish a phase transition which has been experimentally verified for CNTs/hexadecane composites [32] and PNIPAM [33]. An electric field can also be used to alter TC via a morphological change. For example, domain wall configurations are changed when adding external electric fields in ferroelectric materials [34,35]. For those non-ferroelectric materials, an electric field changes TC by affecting the phonon group velocity, the bond stiffness, and the crystal symmetry [36,37]. In our model, the thermal properties are modulated by growing h-BN nanorings on top of pristine graphene. The presence of h-BN nanorings makes the structure piezoelectric, however, its crystal symmetry is broken in the presence of a uniaxial electric field. Thus, TC can be altered flexibly by changing the amplitude of the electric field especially along the armchair direction. In comparison to other tuning methods, mechanical properties are not sacrificed via the application of an electric field. In addition, electric field modulation is quick and repeatable which is of high practical importance for applications.

5. Conclusions

In this contribution we discussed a yet unseen approach to alter the thermal coefficient in pristine graphene by growing an array of h-BN nanorings on top of it. At room temperature, our simulations display how this coefficient can be reduced by 76% thanks to phonon localization comprising rapidly decaying heat currents. We also show how an electric field can be used to significantly tune TC of h-BN nanoring structured graphene due to the structure's piezoelectricity. Using this approach, graphene photonics and optoelectronics could potentially acquire longer propagation lengths and higher efficiency through reduced thermal dissipation.

Author contributions

Dan Tan: Methodology, Data analysis; Morten Willatzen: Formal analysis, Investigation; Johan Christensen: Conceptualization. All authors made contributions to the writing, review and editing of the manuscript.

Declaration of competing interest

The authors declare that they have no known competing financial interests or personal relationships that could have appeared to influence the work reported in this paper.

Data availability

No data was used for the research described in the article.

Acknowledgements

This research is supported by the National Natural Science Foundation of China (Grant No. 12002054) and Qin Chuang Yuan cited high-level innovation and entrepreneurship talent project (Grant No. QCYRCXM-2022-37). Useful discussions with Dr. Pu Zhang and Dr. Weihua Wang are gratefully acknowledged.

Appendix A. Supplementary data

Supplementary data to this article can be found online at https://doi.org/10.1016/j.jpcs.2023.111414.

References

[1] K.S. Novoselov, A.K. Geim, S.V. Morozov, D. Jiang, Y. Zhang, S.V. Dubonos, I. V. Grigorieva, A.A. Firsov, Electric field effect in atomically thin carbon films, Science 306 (2004) 666–669.
[2] C. Berger, Z. Song, X. Li, X. Wu, N. Brown, C. Naud, D. Mayou, T. Li, J. Hass, A. N. Marchenkov, E.H. Conrad, P.N. First, W.A. de Heer, Electronic confinement and coherence in patterned epitaxial graphene, Science 312 (2006) 1191–1196.
[3] R.R. Nair, P. Blake, A.N. Grigorenko, K.S. Novoselov, T.J. Booth, T. Stauber, N.M. R. Peres, A.K. Geim, Fine structure constant defines visual transparency of graphene, Science 320 (2008), 1308–1308.
[4] F. Bonaccorso, Z. Sun, T. Hasan, A.C. Ferrari, Graphene photonics and optoelectronics, Nat. Photonics 4 (2010) 611–622.
[5] L.M. Malard, M.A. Pimenta, G. Dresselhaus, M.S. Dresselhaus, Raman spectroscopy in graphene, Phys. Rep. 473 (2009) 51–87.
[6] A.K. Geim, K.S. Novoselov, The rise of graphene, Nat. Mater. 6 (2007) 183–191.
[7] J. Christensen, A. Manjavacas, S. Thongrattanasiri, F.H.L. Koppens, F.J. García de Abajo, Graphene plasmon waveguiding and hybridization in individual and paired nanoribbons, ACS Nano 6 (2012) 431–440.
[8] J.C.W. Song, N.M. Gabor, Electron quantum metamaterials in van der Waals heterostructures, Nat. Nanotechnol. 13 (2018) 986–993.
[9] M. Yankowitz, Q. Ma, P. Jarillo-Herrero, B.J. LeRoy, van der Waals heterostructures combining graphene and hexagonal boron nitride, Nat. Rev. Phys. 1 (2019) 112–125.
[10] S. Ghosh, I. Calizo, D. Teweldebrhan, E.P. Pokatilov, D.L. Nika, A.A. Balandin, W. Bao, F. Miao, C.N. Lau, Extremely high thermal conductivity of graphene: prospects for thermal management applications in nanoelectronic circuits, Appl. Phys. Lett. 92 (2008), 151911.
[11] A.A. Balandin, S. Ghosh, W. Bao, I. Calizo, D. Teweldebrhan, F. Miao, C.N. Lau, Superior thermal conductivity of single-layer graphene, Nano Lett. 8 (2008), 902–7.
[12] S. Chen, Q. Wu, C. Mishra, J. Kang, H. Zhang, K. Cho, W. Cai, A.A. Balandin, R. S. Ruoff, Thermal conductivity of isotopically modified graphene, Nat. Mater. 11 (2012), 203–7.
[13] M. Nomura, R. Anufriev, Z. Zhang, J. Maire, Y. Guo, R. Yanagisawa, S. Volz, Review of thermal transport in phononic crystals, Mater. Today Phys 22 (2022), 100613.
[14] E.S. Landry, M.I. Hussein, A.J.H. McGaughey, Complex superlattice unit cell designs for reduced thermal conductivity, Phys. Rev. B 77 (2008), 184302.
[15] T. Zhu, E. Ertekin, Phonon transport on two-dimensional graphene/boron nitride superlattices, Phys. Rev. B 90 (2014), 195209.
[16] S. Xiong, K. Sääskilahti, Y.A. Kosevich, H. Han, D. Donadio, S. Volz, Blocking phonon transport by structural resonances in alloy-based nanophononic metamaterials leads to ultralow thermal conductivity, Phys. Rev. Lett. 117 (2016), 025503.
[17] J. Maire, R. Anufriev, R. Yanagisawa, A. Ramiere, S. Volz, M. Nomura, Heat conduction tuning by wave nature of phonons, Sci. Adv. 3 (2017) 1–7.
[18] P. Xiao, E. Chavez-Angel, S. Chaitoglou, M. Sledzinska, A. Dimoulas, C. M. Sotomayor Torres, A. El Sachat, Anisotropic thermal conductivity of crystalline layered SnSe 2, Nano Lett. 21 (2021), 9172–9.
[19] S. Jung, M. Park, J. Park, T.-Y. Jeong, H.-J. Kim, K. Watanabe, T. Taniguchi, D. H. Ha, C. Hwang, Y.-S. Kim, Vibrational properties of h-BN and h-BN-graphene heterostructures probed by inelastic electron tunneling spectroscopy, Sci. Rep. 5 (2015), 16642.
[20] X. Meng, J. Zhang, J. Ma, Y. Li, Z. Chen, S. Liu, T. Chen, Y. Zhang, X. Jiang, S. Zhu, Using cellulose nanocrystals for graphene/hexagonal boron nitride nanosheet films towards efficient thermal management with tunable electrical conductivity, Composer Part A Appl. Sci. Manuf. 138 (2020), 106089.
[21] M. Yankowitz, J. Jung, E. Laksono, N. Leconte, B.L. Chittari, K. Watanabe, T. Taniguchi, S. Adam, D. Graf, C.R. Dean, Dynamic band-structure tuning of graphene moiré superlattices with pressure, Nature 557 (2018) 404–408.
[22] Y. He, G. Galli, Microscopic origin of the reduced thermal conductivity of silicon nanowires, Phys. Rev. Lett. 108 (2012), 215901.
[23] C. Carbogno, R. Ramprasad, M. Scheffler, Ab initio green-kubo approach for the thermal conductivity of solids, Phys. Rev. Lett. 118 (2017), 175901.
[24] S. Plimpton, Fast parallel algorithms for short-range molecular dynamics, J. Comput. Phys. 117 (1995) 1–42.
[25] J. Tersoff, Modeling solid-state chemistry: interatomic potentials for multicomponent systems, Phys. Rev. B 39 (1989), 5566–8.
[26] A. Kınacı, J.B. Haskins, C. Sevik, T. Çağın, Thermal conductivity of BN-C nanostructures, Phys. Rev. B 86 (2012), 115410.
[27] W. Ouyang, I. Azuri, D. Mandelli, A. Tkatchenko, L. Kronik, M. Urbakh, O. Hod, Mechanical and tribological properties of layered materials under high pressure: assessing the importance of many-body dispersion effects, J. Chem. Theor. Comput. 16 (2020) 666–676.
[28] W. Ouyang, D. Mandelli, M. Urbakh, O. Hod, Nanoserpents: graphene nanoribbon motion on two-dimensional hexagonal materials, Nano Lett. 18 (2018) 6009–6016.
[29] Z. Fan, L.F.C. Pereira, H.-Q. Wang, J.-C. Zheng, D. Donadio, A. Harju, Force and heat current formulas for many-body potentials in molecular dynamics simulations with applications to thermal conductivity calculations, Phys. Rev. B 92 (2015), 094301.
[30] A. Govind Rajan, M.S. Strano, D. Blankschtein, Ab initio molecular dynamics and lattice dynamics-based force field for modeling hexagonal boron nitride in mechanical and interfacial applications, J. Phys. Chem. Lett. 9 (2018) 1584–1591.

[31] J. Shin, J. Sung, M. Kang, X. Xie, B. Lee, K.M. Lee, T.J. White, C. Leal, N.R. Sottos, P.V. Braun, D.G. Cahill, Light-triggered thermal conductivity switching in azobenzene polymers, Proc. Natl. Acad. Sci. U.S.A. 116 (2019), 5973–8.
[32] P.C. Sun, Y.L. Wu, J.W. Gao, G.A. Cheng, G. Chen, R.T. Zheng, Room temperature electrical and thermal switching CNT/hexadecane composites, Adv. Mater. 25 (2013) 4938–4943.
[33] C. Li, Y. Ma, Z. Tian, Thermal switching of thermoresponsive polymer aqueous solutions, ACS Macro Lett. 7 (2018), 53–8.
[34] B.M. Foley, M. Wallace, J.T. Gaskins, E.A. Paisley, R.L. Johnson-Wilke, J.W. Kim, P. J. Ryan, S. Trolier-Mckinstry, P.E. Hopkins, J.F. Ihlefeld, Voltage-controlled bistable thermal conductivity in suspended ferroelectric thin-film membranes, ACS Appl. Mater. Interfaces 10 (2018) 25493–25501.
[35] J.F. Ihlefeld, B.M. Foley, D.A. Scrymgeour, J.R. Michael, B.B. McKenzie, D. L. Medlin, M. Wallace, S. Trolier-Mckinstry, P.E. Hopkins, Room-temperature voltage tunable phonon thermal conductivity via reconfigurable interfaces in ferroelectric thin films, Nano Lett. 15 (2015), 1791–5.
[36] Y. Quan, S.-Y. Yue, B. Liao, Electric field effect on the thermal conductivity of wurtzite GaN, Appl. Phys. Lett. 118 (2021), 162110.
[37] S. Deng, J. Yuan, Y. Lin, X. Yu, D. Ma, Y. Huang, R. Ji, G. Zhang, N. Yang, Electric-field-induced modulation of thermal conductivity in poly(vinylidene fluoride), Nano Energy 82 (2021), 105749.